

Structural and transport characterization of ultra thin Ba_{0.05}Sr_{0.95}TiO₃ layers grown over Nb electrodes for the development of Josephson junctions

M. Sirena, L. Avilés Félix, G. A. Carvacho Vera, H. L. Navarro Fernández, L. B. Steren et al.

Citation: *Appl. Phys. Lett.* **100**, 012602 (2012); doi: 10.1063/1.3675332

View online: <http://dx.doi.org/10.1063/1.3675332>

View Table of Contents: <http://apl.aip.org/resource/1/APPLAB/v100/i1>

Published by the [American Institute of Physics](#).

Related Articles

The morphology of Al-based submicron Josephson junction
J. Appl. Phys. **110**, 123903 (2011)

Josephson Hall current in a noncentrosymmetric superconductor/ferromagnet/superconductor junction
J. Appl. Phys. **110**, 113717 (2011)

Lateral imaging of the superconducting vortex lattice using Doppler-modulated scanning tunneling microscopy
Appl. Phys. Lett. **99**, 192505 (2011)

Spectral characteristics of noisy Josephson flux flow oscillator
J. Appl. Phys. **110**, 053922 (2011)

Quantum crossover in moderately damped epitaxial NbN/MgO/NbN junctions with low critical current density
Appl. Phys. Lett. **99**, 062510 (2011)

Additional information on *Appl. Phys. Lett.*

Journal Homepage: <http://apl.aip.org/>

Journal Information: http://apl.aip.org/about/about_the_journal

Top downloads: http://apl.aip.org/features/most_downloaded

Information for Authors: <http://apl.aip.org/authors>

ADVERTISEMENT

**AIP**Advances

Submit Now

**Explore AIP's new
open-access journal**

- **Article-level metrics
now available**
- **Join the conversation!
Rate & comment on articles**

Structural and transport characterization of ultra thin $\text{Ba}_{0.05}\text{Sr}_{0.95}\text{TiO}_3$ layers grown over Nb electrodes for the development of Josephson junctions

M. Sirena,^{1,(a),b)} L. Avilés Félix,¹ G. A. Carvacho Vera,² H. L. Navarro Fernández,² L. B. Steren,^{3,b)} R. Bernard,⁴ J. Briático,⁴ N. Bergeal,⁵ J. Lesueur,⁵ and G. Faini⁶

¹Centro Atómico Bariloche, Instituto Balseiro, CNEA and Universidad Nacional de Cuyo, Av. Bustillo 9500, 8400 Bariloche, Rio Negro, Argentina

²Universidad de Concepción Facultad de Ciencias Físicas y Matemáticas, Victoria 631, 2613 Concepción, Chile

³Centro Atómico Constituyentes, Av. Gral. Paz 1499, San Martín 1650, Buenos Aires, Argentina

⁴Unité Mixte de Physique CNRS/Thales, Université Paris Sud 11, F-91767 Palaiseau Cedex, France

⁵UPR5-LPEM-CNRS, Physique Quantique, E.S.P.C.I., 10 Rue Vauquelin, 75231 Paris, France

⁶LPN-CNRS, Route de Nozay, 91460 Marcoussis, France

(Received 2 December 2011; accepted 10 December 2011; published online 5 January 2012)

A phenomenological approach was used to obtain critical information about the structure and electrical properties of ultra thin $\text{Ba}_{0.05}\text{Sr}_{0.95}\text{TiO}_3$ (BSTO) layers over Nb electrodes. The method allows, in a simple way, to study and to optimize the growth of the barrier in order to improve the performance and application of Josephson junctions. A very good control of the layer thickness with a low roughness was achieved during the deposition process. The BSTO layers present an energy barrier of 0.6 eV and an attenuation length of 0.4 nm, indicating its good insulating properties for the development of Josephson junctions with improved performance. © 2012 American Institute of Physics. [doi:10.1063/1.3675332]

A Josephson junction (JJ) can be thought as two superconducting layers separated by a thin insulating layer, a normal layer or even a depressed superconducting layer.¹ Due to the proximity effect, Cooper pairs can go through the barrier without any voltage drop across the junction. According to the Josephson equations, if a DC voltage is applied on the junction, the phase shift between the superconducting layers induces an ultra fast AC superconducting current (in the range of 1–1000 GHz).¹ JJ has many technological applications,² e.g., magnetic and bolometric sensors, fabrication of volt standards,³ and ultra-fast microelectronics based in rapid single flux quantum logic. However, the development of complex devices based in Josephson junctions technology is not easy; especially for high transition temperature (high T_c) superconducting materials.⁴ One of the main problems is that in order to fabricate these devices, a large number of JJ must be integrated together and a small dispersion of the junctions' characteristics must be achieved.⁵ Additionally, to overcome the thermal noise and to reduce the devices response time, a high $I_c R_n$ factor (i.e., junction energy) is required, where I_c is the critical current of the junction and R_n its normal resistance. Higher $I_c R_n$ or junction energy can be achieved by reducing the barrier thickness and increasing the effective superconducting coupling across the electrodes. In order to increase the JJ energy and improve the homogeneity of the JJ array, a profound knowledge and control of the insulating barrier must be achieved.

Conductive atomic force microscopy (CAFM) has become an excellent technique to study and characterize insulating barriers for tunneling devices, i.e., magnetic tun-

nel junctions or Josephson junctions. However, even if important research has been done regarding the development of magnetic tunnel junctions^{6–8} and spin filters,⁹ very little work has been done in the study and characterization of insulating barriers for the development of Josephson junctions using CAFM.¹⁰ The characteristics of the barrier, e.g., roughness, energy, and the attenuation length of the current, depend on the electronic properties of the electrodes. Moreover, we have recently found that even substrate roughness can modify the quality of the insulating barrier.¹¹ This indicates that careful measurements of the actual system are needed in order to properly characterize and optimize the barrier properties of the junctions.

Recently, we have used a phenomenological approach to analyze the electrical transport through an insulating barrier in ferromagnetic/insulating bilayers using conducting atomic force microscopy.¹¹ CAFM is proving to be a cost and time efficient way to study these systems compared with junctions fabricated by traditional micro and nano-fabrication methods. However, CAFM typical measurements are done for a voltage tip much higher than the energy barrier, outside the range of standard models and further work in the subject is needed. In this work, the developed method has been applied to the study of superconducting/insulating bilayers. The objective is to validate the method in these systems and to obtain critical information of ultra thin insulating barriers for the development of niobium based Josephson junctions.

$\text{Nb}/\text{Ba}_{0.95}\text{Sr}_{0.05}\text{TiO}_3$ (Nb/BSTO) bilayers were grown on single crystal (100) Si substrates by DC and radio frequency (RF) magnetron sputtering from stoichiometric metallic and ceramic targets. The deposition of the samples was made at room temperature in an Ar atmosphere of 10 mTorr. A RF power of 6.4 W/in.² was used in order to obtain a low deposition rate and improve the control and quality of the insulating barrier. The chamber pressure before deposition was

^{a)} Author to whom correspondence should be addressed. Electronic mail: martin.sirena@hotmail.com.

^{b)} Also at The Argentine National Scientific and Technical Research Council (CONICET).

decreased to $\sim 1 \times 10^{-7}$ Torr in order to reduce the density of impurities in the Nb electrode and to optimize its superconducting transition temperature. Bilayers were fabricated with a BSTO layer thickness ranging from 0.5 nm to 2.5 nm, grown over a niobium electrode with a thickness of 100 nm. The nominal thicknesses of the insulating and the superconducting layers were established by a calibration of the different deposition rates and controlling the deposition time. Niobium films are type II superconductors with a transition temperature of 9.25 K (Ref. 12), and BSTO is a ferroelectric insulator. However, due to the low deposition temperature, the BSTO layer is amorphous.

CAFMs measurements were done in a Veeco Dimension 3100[®] scanning probe microscope with a CAFM module, using a boron doped diamond conductive tip in contact mode. The probe polarization voltage was changed between 1.25 V and 6 V for all the samples, and the same pressure during the scan was used, i.e., the same deflection set point (0.5 V) was used. Different probe polarizations and deflection set points were used to verify that the basic results do not depend on the measurements conditions. $I(V)$ curves of the bilayers with different barrier thicknesses were obtained by CAFM in the “ramp” mode, in which the microscope does not scan the x-y position (in-plane movement), but it holds the tip steady in contact with the surface of the samples. The microscope “scans” the applied tip voltage and measures the current for the different voltages. Several scans are made and averaged in order to reduce noise and to decrease the effect of electrical contact problems.

Figure 1 shows the topographic (left) and CAFM (right) images of the Nb/BSTO bilayers for different thicknesses of the insulating layer. The samples present a low roughness (~ 0.5 nm) and a low density of surface defects (~ 0.01 def/ μm^2). The low density of surface defects is important to reduce the probability of short-circuits between the superconducting electrodes. BSTO layers present very good insulating properties, and no current hot-spots or pinholes were found for thicknesses greater than 0.8 nm, indicating a good covering of the electrodes for these thicknesses. The mean tunneling current decreases as the thickness of the insulating layer increases. CAFM images present an important distribution of the tunneling current, which is typical for these systems and it is generally ascribed to a distribution of the barrier thickness.^{7,11,13}

Figure 2 presents the current-voltage ($I(V)$) characteristic of the bilayers. The experimental data were fitted using the phenomenological model:¹¹

$$\text{Ln}(I(V, d)) = A_0(d) + \alpha(d) \cdot \text{Ln}(V), \quad (1)$$

where A_0 and α depend linearly with the barrier thickness (d), Eq. (1) can be rewritten as

$$\text{Ln}[I(V, d)] = (a_0 + a' \cdot d) + (\alpha_0 + \alpha' \cdot d) \cdot \text{Ln}(V),$$

$$I = e^{a_0} V^{\alpha_0} e^{-\frac{d}{\lambda}}, \quad \text{with} \quad \lambda = \frac{1}{|a'| - \alpha' \cdot \text{Ln}(V)}, \quad (2)$$

where λ is the attenuation length of the carriers in the barrier, $a_0 = A_0(d=0)$, $\alpha_0 = \alpha(d=0)$, $a' = \frac{\partial A_0}{\partial d}$, and $\alpha' = \frac{\partial \alpha}{\partial d}$ (it should

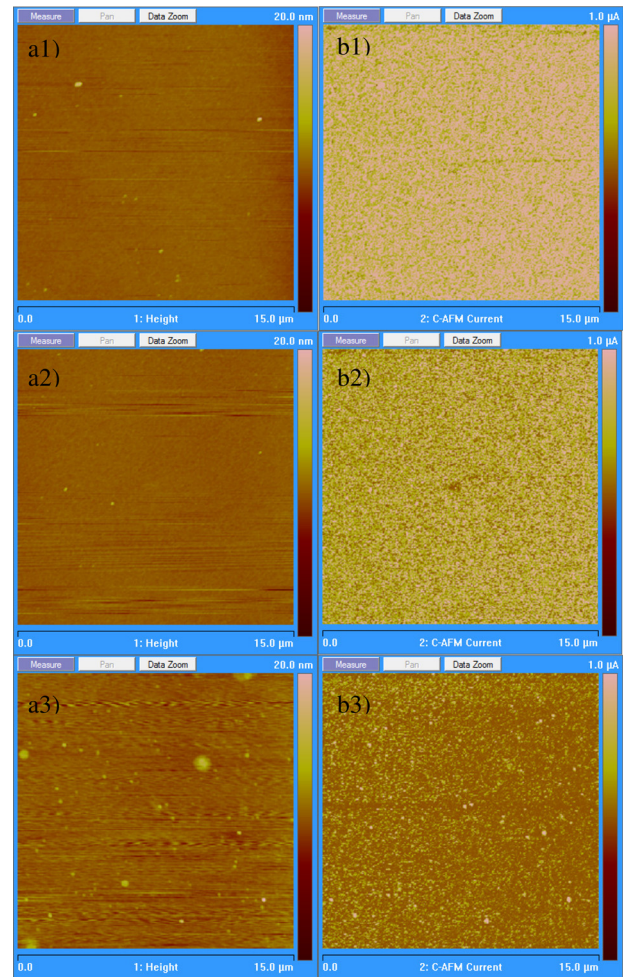


FIG. 1. (Color online) Topographic (left) and CAFM (right) $15 \mu\text{m} \times 15 \mu\text{m}$ images of Nb/BSTO bilayers grown over Si with different BSTO thicknesses (0.67 nm (1), 0.83 nm (2), and 1 nm (3)).

be noted that $a' < 0$). The experimental data show a good agreement with the proposed model. The current decreases exponentially with the barrier thickness, and it presents a potential growth with the applied voltage. The measured

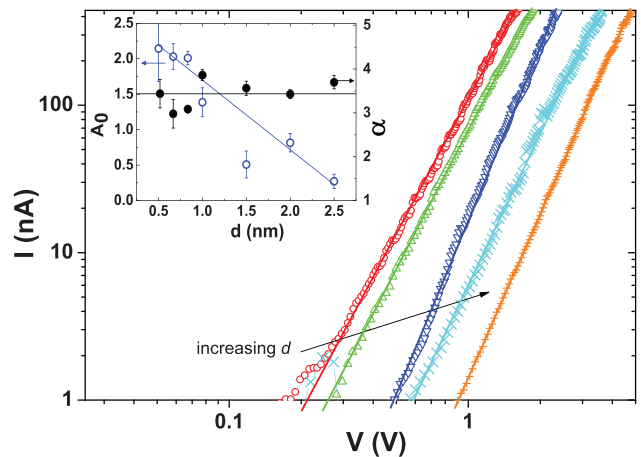


FIG. 2. (Color online) CAFM $I(V)$ curves for the superconducting/insulating bilayers grown over Si. The solid lines are linear fits of the experimental data ($\text{Log}(I) = A_0 + \alpha \cdot \text{Log}(V)$). The inset shows A_0 and α as a function of the barrier thickness (d).

value of α_0 (~ 3.4) is different than $\alpha_0 = 2$, corresponding to the Fowler-Nordheim regime, i.e., high polarization voltages compared with the energy of the barrier.¹⁴ The value of α is consistent with the values obtained for crystalline BSTO layers grown over $\text{La}_{0.75}\text{Sr}_{0.25}\text{MnO}_3$ electrodes.¹¹ However, in contrast with the experimental behavior observed for the crystalline BSTO barrier in ferromagnetic/ferroelectric bilayers, the amorphous BSTO layer present almost no dependence of α with the layer thickness ($\alpha' \approx 0$). Indeed, $I(V)$ curves corresponding to samples with different thicknesses of the BSTO layers are almost parallel. As a consequence, $\alpha' \cdot \ln(V) \approx 0$, and there is no important change of the attenuation length for increasing applied voltage (see Eq. (2)). This could be related to the high applied voltages, much greater than the energy of the barrier. I/V^{α_0} for the bilayers with different thicknesses of the insulating layer was plotted as a function of the applied voltage in a logarithmic scale (Figure 3). In general, no important variation with the applied voltage can be seen, putting in evidence the small change of the carrier attenuation length with the tip polarization voltage (Eq. (2)). This has already been observed for spin filter barriers⁹ and has been ascribed to an experimental artifact originated in the influence of the tip pressure during the measurement and when using the width of the current distribution to calculate λ . The authors conclude that a more reliable method to calculate the attenuation length is to use the decrease of the mean current as a function of the barrier thickness. It is not clear that this is the origin of the observed behavior in our case. Equivalent measurements performed on crystalline BSTO layers show the expected variation of λ with increasing voltage.¹¹ Moreover, the observed behavior in our samples is obtained from the mean current voltage characteristics of the bilayers, measured using different experimental conditions and in different spots on the surface of the sample. More studies in amorphous and crystalline barriers using CAFM and standard macroscopic tunnel junctions are being performed to obtain additional information.

The inset of Figure 3 presents I/V^{α_0} as a function of the barrier thickness measured at 2 V. The experimental data seems to follow the expected linear behavior (Eq. (2)), and

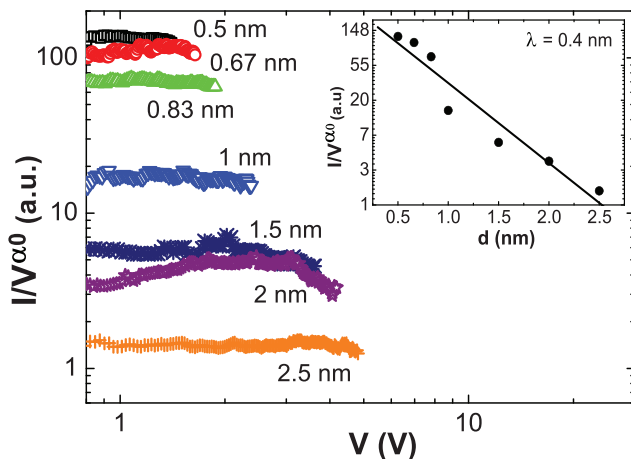


FIG. 3. (Color online) I/V^{α_0} ($\ln(I/V^{\alpha_0}) = a_0 - d/\lambda$) as a function of the polarization voltage for the Nb/BSTO bilayers with different thicknesses of the insulating layer (d). The inset shows I/V^{α_0} as a function of d for a polarization voltage of around 2 V. The line is a linear fit of the experimental data.

the calculated attenuation length for Nb/BSTO bilayers is around 0.4 nm. Considering that in the F-N regime $\frac{1}{\lambda} = \frac{8\pi\sqrt{2}m^*}{3\hbar eV} \phi^{3/2}$,¹⁴ where \hbar is the Planck constant, m^* the effective mass of the current carriers, and V is the applied voltage. Using the calculated value for the attenuation length, the upper limit of the barrier energy is $\phi^{max} \sim 0.6$ eV (considering $m^* =$ electron mass). The values of λ and ϕ^{max} indicate the good insulating quality of the barrier. These values are very similar to the corresponding values of λ (0.35 nm) and ϕ^{max} (0.6 eV) for high quality with low roughness crystalline BSTO barriers grown by sputtering¹¹ or high quality SrTiO_3 barriers grown by pulsed laser deposition.⁷

The I/V^{α_0} distributions for the Nb/BSTO bilayers with different thicknesses of the insulating layer are shown in Figure 4. The lines are the adjusted functions considering a Gaussian distribution for the thickness of the barrier and using the phenomenological model for $I(V, d)$ given by Eq. (2). The only fitting parameter is the barrier roughness, σ_d . The log-normal distribution fits very well the experimental data as expected from previous works.^{7,11,13} A very good insulation of the bottom electrode can be achieved for thicknesses greater than 0.8 nm, with low conductivity values and no presence of pinholes in the barrier. The simulated I/V^{α_0} distributions indicate a low barrier roughness for the tunneling current of 0.36 nm, coherent with the total topographic roughness of the sample (~ 0.5 nm). The experimental data show a very good control of the deposition thickness for ultra-thin BSTO insulating layers over Nb electrodes, with a small barrier roughness. Tunneling seems to be the preferred mechanisms for electrical transport through the barrier.

We have used a phenomenological approach to analyze the electrical transport through ultra-thin BaSrTiO_3 layers grown over Nb electrodes. The proposed method allows, in a simple and direct way, to study and to optimize the growth of insulating barriers over superconductors' electrodes in order to improve the performance and application of Josephson junctions. The tunnelling of the carriers seems to be the main mechanism for electrical transport in these systems, and the BaSrTiO_3 layers present an energy barrier of 0.6 eV with an attenuation length of 0.4 nm, indicating its good insulating properties. The deposition method allows a very

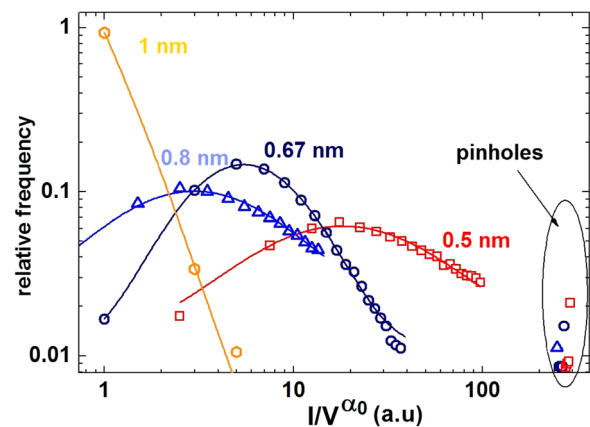


FIG. 4. (Color online) Experimental (open dots) and simulated (lines) I/V^{α_0} distributions for Nb/BSTO bilayers grown over Si, for different BSTO thicknesses.

good control of the barrier thickness. These are promising results for the development of Josephson junctions with improved performance.

M.S. acknowledges K. Bouzehouane and S. Fusil for the formation received in CAFM measurements and Professor L. Bennun and Universidad de Concepción for the students travel support program. The authors would also like to thank R. Benavidez and Ignacio Artola for extraordinary technical support. This work was partially supported by the ANPCYT (PICT PRH 2008-109), Universidad Nacional de Cuyo (06/C328) and the international cooperation program MINCYT-ECOS (France) A10E05.

¹B. D. Josephson, *Phys. Lett.* **1**, 251 (1962).

²S. Anders, M. G. Blamire, F.-I. Buchholz, D.-G. Cr  t  , R. Cristiano, P. Febvre, L. Fritzsche, A. Herr, E. Il'ichev, J. Kohlmann *et al.*, *Physica C* **470**, 2079 (2010).

³C. A. Hamilton, R. L. Kautz, R. L. Steiner, and F. L. Lloyd, *IEEE Electron Device Lett.* **6**, 623 (1985).

⁴N. Bergeal, J. Lesueur, M. Sirena, G. Faini, M. Aprili, and J. P. Contour, *J. Appl. Phys.* **102**, 083903 (2007).

⁵S. A. Cybart, K. Chen, Y. Cui, Q. Li, X. X. Xi, and R. C. Dynes, *Appl. Phys. Lett.* **88**, 012509 (2006).

⁶K. M. Bhutta, J. Schmalhorst, and G. Resiss, *J. Magn. Magn. Mater.* **321**, 3384 (2009).

⁷T. Fix, V. Da Costa, C. Ulhaq-Bouillet, S. Colis, A. Dinia, K. Bouzehouane, and A. Barth  l  my, *Appl. Phys. Lett.* **91**, 083104 (2007).

⁸I. C. Infante, F. Sanchez, V. Laukhin, A. Perez del Pino, J. Fontcuberta, K. Bouzehouane, S. Fusil, and A. Barth  l  my, *Appl. Phys. Lett.* **89**, 172506 (2006).

⁹M. Foerster, F. Rigato, K. Bouzehouane, and J. Fontcuberta, *J. Phys. D: Appl. Phys.* **43**, 295001 (2010).

¹⁰K. M. Lang, D. A. Hite, R. W. Simmonds, R. McDermott, P. Pappas, and J. M. Martinis, *Rev. Sci. Instrum.* **75**, 2726 (2004).

¹¹M. Sirena, *J. Appl. Phys.* **110**, 063923 (2011).

¹²D. K. Finnemore, T. F. Stromberg, and C. A. Swenson, *Phys. Rev.* **149**, 231 (1966).

¹³F. Bardou, *Europhys. Lett.* **39**, 239 (1997).

¹⁴J. G. Simmons, *J. Appl. Phys.* **34**, 1793 (1963); *J. Phys. D* **4**, 613 (1971).